Physica Medica 141 (2026) 105701

Contents lists available at ScienceDirect

Physica Medica

journal homepage: www.elsevier.com/locate/ejmp

Performance tests of the B-RAD survey meter and portable γ-spectrometer in a clinical environment

Marco Silari [a,b,*], Marco Brambilla [c], Alessandro Carriero [d], Pierfrancesco Franco [e], Gianfranco Loi [c], Michele Lorenzoli [f], Roberta Matheoud [c]

[a] Politecnico di Milano, via G. La Masa 34, 20156 Milan, Italy
[b] CERN, 1211 Geneva 23, Switzerland
[c] SC Fisica Sanitaria, AOU Maggiore della Carità, C.so Mazzini 18, 28100 Novara, Italy
[d] Radiology Department, AOU Maggiore della Carità, C.so Mazzini 18, 28100 Novara, Italy
[e] Division of Radiation Oncology, AOU Maggiore della Carità, C.so Mazzini 18, 28100 Novara, Italy
[f] ELSE NUCLEAR, Via Riccardo Pitteri 10, 20134 Milan, Italy

A B S T R A C T

Introduction: This note describes performance test of B-RAD, a commercial γ-survey meter/portable γ-spectrometer designed to operate in strong magnetic field. The instrument consists of an active probe housing a cylindrical $LaBr_3$ crystal, and a central unit connected by a cable.
Methods: The measurements were performed at an MR-Linac Elekta Unity (1.5 T) and a Philips Ingenia (3 T) MRI system, by measuring the $H^*(10)$ rate and the gamma energy distributions using two certified radioactive sources of ^{57}Co and ^{137}Cs providing a reference irradiation while the detector was exposed to increasing values of the magnetic field. Measurements were performed in various configurations, with probe and central unit either kept close together or separate, and either aligned or orthogonal to the magnetic field.
Results: The results outline stable $H^*(10)$ rates and gamma spectrometry performances in the entire magnetic field range. The device's performance is unaffected when only the probe is exposed to the static magnetic field while the central unit is in a lower field zone. When the latter is exposed to a strong field, the loss in dose rate remains within 10% for all configurations tested.
Conclusion: The results demonstrate the potential application of the instrument for operational and decommissioning measurements at MRI-Linac and PET-MRI systems.

1. Introduction

This note describes performance tests in a clinical environment of B-RAD, a novel γ-survey meter/portable γ-spectrometer specifically conceived to operate in strong magnetic field. The instrument provides both ambient dose equivalent ($H^*(10)$) rate, with a response linear up to about 20 mSv/h, and isotope identification. It was jointly designed by CERN Radiation Protection group and the Department of Energy of the Polytechnic of Milan (POLIMI), patented [1] and later licenced to a private company to develop an industrial version [2]. The B-RAD has been on the market for about five years.

The B-RAD was designed as hand-held survey meter and γ-spectrometer capable to operate in strong magnetic field, originally for use at the Large Hadron Collider (LHC) experiments at CERN. The requirement was to measure the residual radioactivity around and (in case of ATLAS) inside the large underground detectors without switching the magnetic field off (up to 1 T inside ATLAS). Radiation protection instruments are not designed with such a requirement in mind, and very little information is available in the literature on this topic. There obviously exist detectors conceived to operate inside a magnetic field, such as those employed in high-energy physics experiments or the small detectors used in PET-MRI, but they are integrated into large installations. They are neither stand-alone, portable devices, nor provide – within a single instrument – $H^*(10)$ rates, spectral information and isotope identification. A study on eight survey meters, dated to more than 30 years ago, was limited to 0.03 T field [3]. Before undertaking the development of B-RAD, tests on several commercial survey meters were conducted at CERN in 2010. All instruments failed in magnetic fields below 0.3 T, and several of them showed deficiencies already at 0.1 T [4]. A subsequent investigation in 2018 confirmed these findings [4].

The original B-RAD prototype and earlier tests are described in [4], extensive performance tests conducted at CERN on the industrial version in [5]. The latter include the verification of the linearity of the dose rate response and of the angular response, performance tests up to 1.4 T in a

* Corresponding author at: Politecnico di Milano, via G. La Masa 34, 20156 Milan, Italy.
E-mail address: Marco.Silari@cern.ch (M. Silari).

https://doi.org/10.1016/j.ejmp.2025.105701
Received 17 June 2025; Received in revised form 30 October 2025; Accepted 11 December 2025
Available online 13 December 2025

Fig. 1. The ^{57}Co source (left) and ^{137}Cs source (right) fixed to the B-RAD probe.

calibrated dipole magnet, and one test in a 2.5 T solenoid with an earlier model of the industrial product. An on-the-field test was also performed to demonstrate the use of B-RAD in a practical application, namely the measurement of the weak residual radioactivity in small permanent magnets for their radiological clearance and elimination from CERN.

The scope of the present measurements was to confirm the results – with the latest version of the device – of the earlier tests [4,5]. The purpose was to verify the capability of the B-RAD to operate correctly – both as survey meter and as γ-spectrometer – in a clinical environment up to 3 T field. This study was undertaken is view of the emerging role of hybrid technologies, such as MRI-Linac for image-guided adaptive radiation therapy and PET-MRI for combined imaging applications, which may involve the need of performing radiation measurements in presence of an intense magnetic field, either in operational conditions or for decommissioning. Nonetheless, the instrument can generally find application for radiation monitoring in any process requiring the presence of magnetic fields, such as scrap metal handling or handling of containers using lifting magnets. These radiological measurements are usually not possible with standard commercial γ-monitors.

2. Materials and methods

The B-RAD consists of an active probe (P) connected to a central unit (CU) by a 1 m cable. The probe houses a cylindrical $LaBr_3$ crystal (15 mm diameter × 15 mm height) coupled to a 16-pixel Silicon Photomultiplier (SiPM) ArrayC-30035 from SensL, along with Front-End electronics. The central unit includes the main electronic circuitry, a battery, a double display and a Faraday cage that is used to shield the electronics from external electromagnetic fields. All active components were selected to be insensitive to strong magnetic fields (e.g., using SiPMs instead of a photomultiplier tube, a display with aluminum case, and selecting electronics components with lowest inductance), and the mass of metallic parts kept to the minimum.

The B-RAD dose rate algorithm calculates the $H^*(10)$ rate starting from the gamma spectrum. The base concept is to flatten the energy response to allow using a single dose rate calibration factor. This is obtained by multiplying the counts of each spectrum bin by the corresponding energy and by weights depending on several energy regions; with the combination of these corrections, the maximum variations of the energy response are within 10 %. The weighted counts obtained with the flattening algorithm are then corrected for dead time effects and ultimately integrated and multiplied by the dose rate calibration factor. Considering the dependence on energy of the flattening algorithm, a shift in the spectrum gain that is not corrected by a new energy calibration can result in a significant variation in the $H^*(10)$ rate, especially for higher energies when moving between weighting regions.

The tests were performed at the *Azienda Ospedaliero-Universitaria AOU Maggiore della Carità* in Novara, at the MRI-Linac Elekta Unity (1.5 T) and at the Philips Ingenia (3 T) MRI system, by measuring the $H^*(10)$ rate and the gamma energy distributions using two certified radioactive sources, ^{57}Co (Eγ = 122 keV, A = 8.14 MBq on 16/6/2021, $T_{1/2}$ = 270 days) and ^{137}Cs (Eγ = 662 keV, A = 3.7 MBq on 1/1/1978, $T_{1/2}$ = 30.17 years), at magnetic field intensities ranging from zero to 3 T.

The MRI-Linac Elekta Unity (Elekta AB, Stockholm, Sweden) couples a ring gantry mounted 7 MV standing-wave Linac with an Ingenia 1.5 T MRI scanner (Philips Healthcare, Best, Netherland). The Ingenia MRI sub-system is based on the wide bore Philips Ingenia 1.5 T technology. It consists of an actively shielded 1.5 T superconducting magnet with a 70 cm bore diameter, but, differently from the diagnostic MRI scanner, the B0 and gradient coils are physically split, creating a 22 cm gap around the isocentre to allow the passage of the treatment beam [6]. The MRI system is equipped with a 2 × 4 channel (four anterior, four posterior) receive coil array allowing the execution of the same exam cards available on the parent Ingenia 1.5 T system adjusted and optimized for the Unity operating parameters (maximum gradient strength 15 mT/m, maximum slew rate 65 T/m/s).

The Ingenia 3.0 T CX (Philips Healthcare) is a superconductive MRI system with a 50 cm axial field of view and a 60 cm bore, equipped with dual gradients (maximum amplitude on each axis 80 mT/m, maximum slew rate 200 T/m/s), parallel radiofrequency transmission and digital body coil. Additional coils as flex coverage posterior, total spine, head/neck, torso, total body, knee and breast allow to perform all clinical examinations in standard and advanced imaging modalities [7,8].

Each radioactive source was in turn attached to the B-RAD probe (Fig. 1), close to the $LaBr_3$ sensitive volume, to provide a reference $H^*(10)$ rate while the detector was exposed to increasing values of the magnetic field. Measurements from zero static magnetic field to 1.5 T were performed at the MRI-Linac on 18 September 2024, while measurements from 1.5 T to 3 T were made at the MRI system on 28 January 2025. Four configurations were tested at the MRI-Linac, whereas measurements in the 1.5 T to 3 T range at the MRI system could only be performed in two configurations, as discussed below. For each measurement, the magnetic field intensity at the locations of both probe and central unit was measured with a Metrolab ETM-1 3-axis hall teslameter with measuring range 0 – 2 T [9].

The spectra associated with each value of the $H^*(10)$ rate were all recorded. The 122 keV peak of ^{57}Co and the 662 keV peak of ^{137}Cs in the spectra obtained in absence of magnetic field were used as reference to recalculate the energy calibrations for the respective measurement campaigns. By reprocessing the $H^*(10)$ rate of the newly calibrated spectra, minor variations in dose rate were obtained for the September 2024 measurements with both sources, and for the January 2025 measurements with ^{57}Co, while the correction of the ^{137}Cs January measurements was more substantial and resulted in an alignment of the new dose rates with those previously obtained during the September measurements.

To combine the two sets of measurements of September 2024 and January 2025 with the ^{57}Co source, the measured $H^*(10)$ rates were corrected for the 132-day decay from the measurements at the MRI-Linac to the date of the measurements at the MRI system. Considering the 30 years half-life of ^{137}Cs, for this source the decrease in dose rate

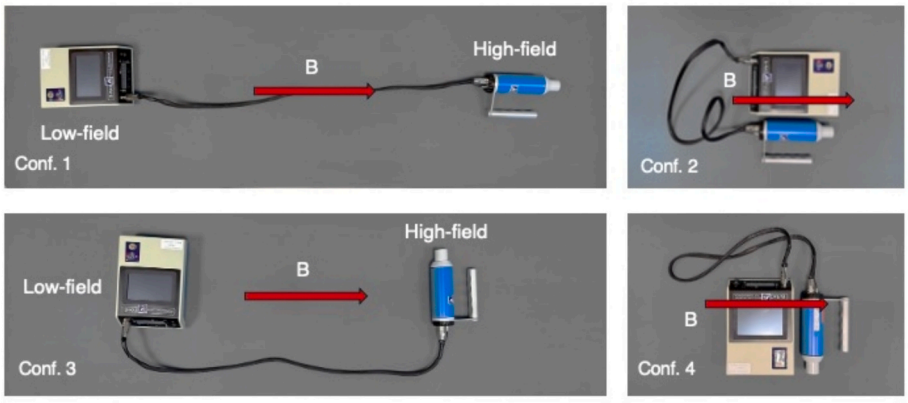

Fig. 2. The four configurations in which the B-RAD was tested at the MRI-Linac and at the MRI system.

between the two sets of measurements is negligible and no correction was applied.

2.1. Measurements at the MRI-Linac

The B-RAD was placed on the axis of the couch and progressively moved towards region of increasing magnetic field, up to the maximum value of 1.5 T inside the bore. The instrument was tested in four configurations (Fig. 2):

1) Probe (P) and central unit (CU) kept separate, with P inside the higher field region and the CU about 1 m back (the length of the cable), in a lower-field zone. P and CU *aligned* with the magnetic field (i.e. P and CU axes aligned with the couch axis).
2) P and CU kept together, *aligned* with the magnetic field.
3) P and CU kept separate, with P inside the higher field region and CU a bit less than 1 m back in lower-field zone. P and CU placed *orthogonal* to the magnetic field (i.e. P and CU axes orthogonal to the couch axis).
4) P and CU kept together (P in front, in higher field than CU), *orthogonal* to the magnetic field.

It should be underlined that for the confs. 2) and 4), in which P and CU were kept together, inside the bore the field gradient is very steep: the intensity of the B field at the position of the CU was approximately half than at the position of the P.

The first measurement with each source was made in zero magnetic field region (i.e., outside the Linac room). The $H^*(10)$ rate reported is the value averaged over a measurement time of 30 s.

2.2. Measurements at the MRI system

The radioactive source was attached to the probe as in the previous measurements at the MRI-Linac. The B-RAD was placed on the axis of the couch and moved from the position in which the probe was in about 1.5 T field to locations in which the field at the probe was about 2 T and 3 T (in the middle of the bore). Measurements between 2 T and 3 T were not performed because the ETM-1 teslameter operating range is limited to 2 T. The measurement at 1.5 T was done to match the results obtained at the MRI-Linac.

Measurements could only be performed for configurations 1 and 3 listed in section 2.1. Measurements in the configurations with P and CU kept together could not be made because the force exerted by the magnetic field on the CU was too strong and could have posed a risk to the MRI system. As for the MRI-Linac measurements, the first measurement was made outside the MRI system room, in zero magnetic field

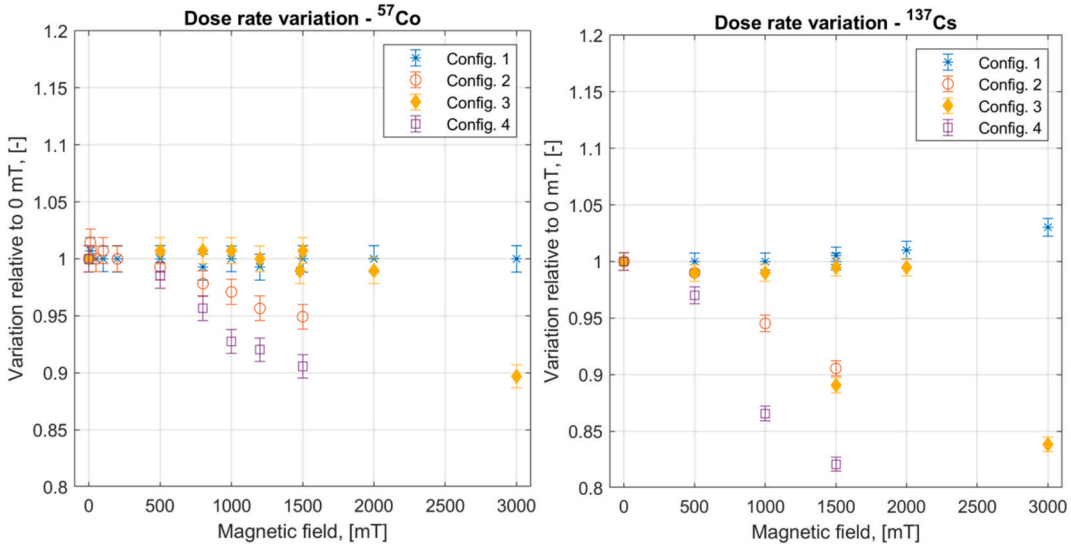

Fig. 3. Relative variation of the B-RAD dose rate with the ^{57}Co source (left plot) and ^{137}Cs source (right plot) fixed to the probe, as a function of magnetic field intensity, for the four configurations described in section 2.1. Measurements in configurations 2 and 4 could only be performed up to 1.5 T, as explained in the text. The error bars are the statistical uncertainties.

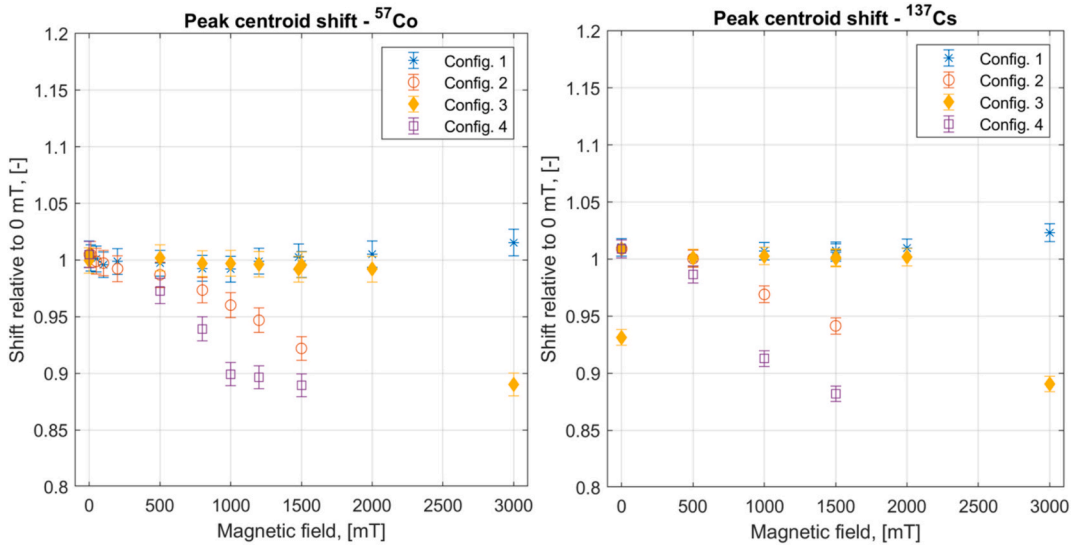

Fig. 4. Relative variation of the position of the ^{57}Co (left plot) and ^{137}Cs (right plot) photoelectric peaks as a function of magnetic field intensity, for the four configurations described in section 2.1. Measurements in configurations 2 and 4 could only be performed up to 1.5 T, as explained in the text. The error bars are the statistical uncertainties.

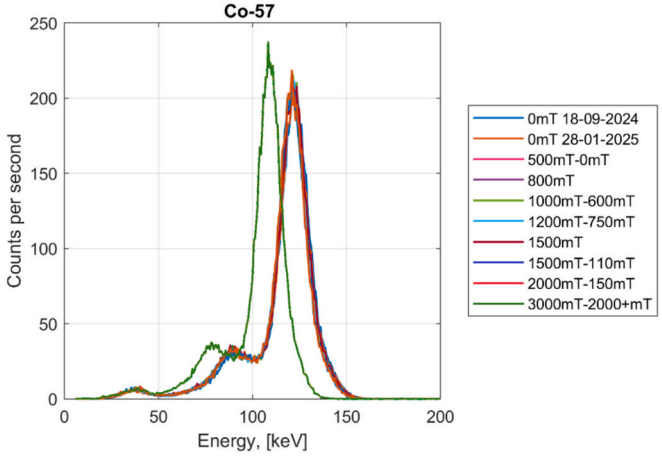

Fig. 5. Shift in the ^{57}Co spectrum and in the position of the photoelectric peak as a function of magnetic field intensity, for conf. 3: P inside the higher field region and CU about 1 m back in lower-field zone, both *orthogonal* to the magnetic field. The legend gives the value of B at the P and CU positions. Two measurements were performed at zero field and at 1.5 T, in September 2024 and in January 2025. At 0.8 T and for one of the measurements at 1.5 T the field at the CU position was not noted.

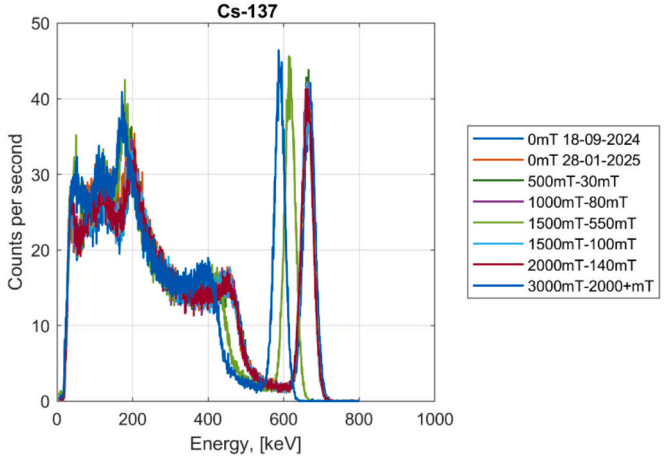

Fig. 6. Shift in the ^{137}Cs spectrum and in the position of the photoelectric peak as a function of magnetic field intensity, for conf. 3: P inside the higher field region and CU about 1 m back in lower-field zone, both *orthogonal* to the magnetic field. The legend gives the value of B at the P and CU positions. Two measurements were performed at zero field and at 1.5 T, in September 2024 and in January 2025.

region.

3. Results and discussion

Fig. 3 plots the relative variation of the dose rate as a function of magnetic field intensity, normalised to the value measured in absence of magnetic field, for the four configurations described above. With only the probe in the high-field region, *aligned* with the magnetic field (conf. 1), the response of the B-RAD does not change up to 3 T (the 3 % increase seen at 3 T with the ^{137}Cs source, which is slight outside the statistical uncertainties, is currently unexplained. A detailed analysis of the electronic chain of the instrument was performed, but no component was identified that could affect the system and explain this behaviour). With the probe placed *orthogonal* to the magnetic field (conf. 3), the response at 3 T is about 10 % and 15 % lower than at zero field with the ^{57}Co and ^{137}Cs sources, respectively. For configurations 2 and 4 in which P and CU are kept close together, the response slowly drops with increasing B-field: at 1.5 T it is 90–95 % of the reference value at zero field with the ^{57}Co source, and 82–90 % with the ^{137}Cs source. The magnetic field has a clear, albeit small influence on the central unit and practically no influence on the probe. The orientation of the central unit, *aligned* or *orthogonal* to the magnetic field, also has a slight influence on the instrument response. As previously reported, the measurements at 1.5 T for confs. 1 and 3 were repeated to match the data collected at the two scanners. The discrepancy between the two values arises from the different stray field at the position of the CU. The intensity of the stray field was 100 mT on the MRI system and 500 mT on the MRI-Linac, respectively. The difference is particularly evident for the ^{137}Cs source with the lower value corresponding to the higher stray field. Anyhow, the deviations are sufficiently small to be included in the overall uncertainty of the reading for this type of measurement.

This trend in the dose rate is explained by the fact that it is calculated from the gamma spectrum, as explained in section 2. Fig. 4 shows the

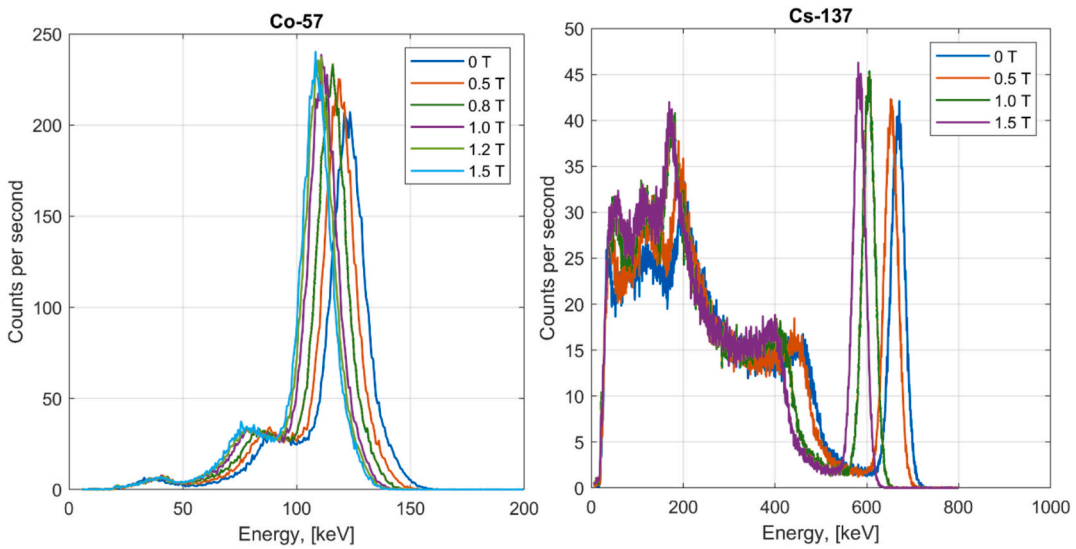

Fig. 7. Shift in the ^{57}Co (left plot) and ^{137}Cs (right plot) spectra and in the position of the photoelectric peaks as a function of magnetic field intensity, for conf. 4: P and CU kept together, *orthogonal* to the magnetic field.

relative variation of the position of the ^{57}Co and ^{137}Cs photoelectric peaks as a function of magnetic field intensity. The trends reproduce those of the dose rates in Fig. 3. Fig. 5 and Fig. 6 show the shift in the ^{57}Co and ^{137}Cs spectra and in the position of the photoelectric peaks as a function of magnetic field intensity, for conf. 3, with P inside the higher field region and CU placed back in a lower-field zone. The shift in the spectra only becomes noticeable above 1.5 T. Finally, Fig. 7 shows the shift in the ^{57}Co and ^{137}Cs spectra and in the position of the photoelectric peaks as a function of magnetic field intensity, for conf. 4, in which P and CU are kept together. With the central unit in the high-field region, the spectra progressively shift to the left with increasing field.

The way in which the algorithm calculates the $H^*(10)$ rate from the gamma spectrum, illustrated in section 2, explains why the decrease in dose rate with increasing B is different for the two sources. Whereas the integral of the spectrum does not change, at higher fields part of the counts moves from the region above about 300 keV, where the weigh for calculating $H^*(10)$ is 1.1, to the 50–300 keV region, where the weigh is 0.33. Most of the ^{57}Co spectrum lies between 60 keV and 160 keV, so the shifting of the spectrum to the left does not move the spectrum between weighting regions and the calculated dose rate decrease follows the peak shifting. In the ^{137}Cs spectrum, on the other hand, the shifting of the Compton distribution and backscattering peak to the left causes an increase on the counts falling below 300 keV rather than above this threshold. For this reason, an increasing portion of the spectrum is multiplied by the lower weight, causing a decrease of the calculated dose rate that is faster than the photopeak shifting to the left. As mentioned above, the integral counts of the spectra are not affected by the magnetic field variation, therefore no effect on dead time was identified.

It should be noted that measurements in the presence of gamma emitters with energies higher than that of ^{137}Cs are not substantially affected. As seen, the difference in the dose rate variation of ^{137}Cs in respect of that of ^{57}Co depends on the increasing number of counts in the backscattering area. This is below the 300 keV threshold, so it is given a lower weight by the algorithm, which is not an issue for the ^{57}Co spectrum being all below 200 keV. For higher energy sources the backscattering energy presents small variations, so the effect on the overall dose rate calculation does not worsen in respect of ^{137}Cs.

It should also be mentioned that during the B-RAD development, the feasibility of integrating a three-axes Hall sensor in the probe was considered, to establish a correction curve based on the measured magnetic field and compensate for the systematic error in the dose rate determination. This solution was finally deemed not necessary, as it has been demonstrated that the variation of the reading with magnetic field is well within the uncertainty acceptable for radiation protection instrumentation.

The present results are consistent with those reported in [5] and extend them to 3 T.

4. Conclusions

The present results have confirmed the capability of B-RAD to operate correctly in magnetic field up to 3 T, providing reliable $H^*(10)$ measurements and spectra identification. The performance is nearly unaffected when only the probe is exposed to the static magnetic field while the central unit is in a lower field zone. This is expected to be the case for most practical situations, as it is logical to assume that the central unit will be kept close to the operator (e.g., carried at the waist). The slight loss in dose rate with increasing field remains within about 10 % for all configurations tested, which is fully acceptable for radiation protection purposes. The spectrum acquisition and radioisotope identification are also not affected, making the B-RAD a unique instrument amongst survey meters and gamma spectrometers.

Declaration of competing interest

The authors declare the following financial interests/personal relationships which may be considered as potential competing interests: One of the authors (MS) is one of the inventors and holds a patent, but he has no shares in ELSE NUCLEAR and receives no royalties from the commercialization of the B-RAD. Another author (ML) is an ELSE NUCLEAR employee, but he does not receive any additional financial benefit from the commercialization of the B-RAD on top of his salary.

Acknowledgements

The authors wish to thank Gabriele Zorloni and Marcello Ballerini of ELSE NUCLEAR for useful discussions on the experimental results.

References

[1] Fazzi A, Silari M. Portable radiation detection device for operation in intense magnetic fields. CERN/ Polytechnic of Milan joint patent. Patent Grant number 9977134, 2017, 13.
[2] ELSE NUCLEAR, Hand-held spectrometer for gamma radiation, http://www.elsenuclear.com/en/b-rad [accessed 20 October 2025].

[3] Liu JC, Mao S, McCall RC, Donahue R. The effect of static magnetic field on the response of radiation survey instruments. Health Phys 1993;64:59–63. https://doi.org/10.1097/00004032-199301000-00007.
[4] Celeste D, Curioni A, Fazzi A, Silari M, Varoli V. B-RAD: a radiation survey meter for operation in intense magnetic fields. JINST 2019;14:T05007. https://doi.org/10.1088/1748-0221/14/05/T05007.
[5] Ferrulli F, Silari M. Performance tests of the B-RAD radiation survey meter. Nuclear Inst and Methods A 2022;1042:167430. https://doi.org/10.1016/j.nima.2022.167430.
[6] Tijssen RHN, et al. MRI commissioning of 1.5T MRI-linac systems - a multi-institutional study. Radiother Oncol 2019;132:114–20. https://doi.org/10.1016/j.radonc.2018.12.011.
[7] https://images.philips.com/is/content/PhilipsConsumer/Campaigns/HC20140401_DG/Documents/452299108541_LR_ingenia_3TCX%20brochure.pdf [accessed 20 October 2025].
[8] Manual Koninklinijke Philips N.V. 2017.
[9] Metrolab ETM-1 Teslameter. https://www.gruppompb.com/public/upload/ETM-1.pdf.